Finite element solution of an elastically connected double Bernoulli-Euler beam system on Winkler-Kerr foundation

Welky Klefson Ferreira de Brito[1], Arthur Coutinho de Araújo Pereira[1], Ângelo Vieira Mendonça[1]

[1]*Universidade Federal da Paraíba - UFPB*
Cidade Universitária, 58051-900, João Pessoa/PB, Brasil
klefsonbrito@hotmail.com

Abstract. In the last decades, studies on the double-beam system, which consists of two parallel beams connected by an elastic layer, have been focus of much researches and applied to a wide variety of engineering problems such as, adhesively bonded joints, rail on geocell-reinforced earth bed and many others. Different models of one, two and three parameters have been used to represent the inner connecting layer of the beams and the support base. In this paper, a finite element formulation is derived assuming the Euler-Bernoulli beam hypotheses to represent the beams, the Winkler foundation model to idealize the inner layer, and the Kerr elastic foundation assumptions to model the support base. The double beam finite element has ten degrees of freedom and its stiffness matrix and equivalent load vector are explicitly shown. Numerical bending analysis for many different load cases, beam properties, and foundation parameters is done and compared with analytical solution or numerical responses, according to their availabilities.

Keywords: Double-beam system, FEM, Winkler-Kerr foundation.

1 Introduction

The variety of applications of the elastically connected double-beam system (DBS) has drawn the attention of several researchers once DBS can be used to modelled a lot of problems on civil, aerospace and mechanical engineering. The DBS as a complex continuous system consisting of two parallel solids joined by an elastic medium treated through beams theories combined with elastic layers models, avoiding to use rigorous models based on elasticity theory to represent all interaction forces and stresses at interfaces beam-layer-beam.

Based on the Bernoulli-Euler theory, several studies can be found in the literature such as free and/or forced vibration problems ([1] -[11]), buckling problems [12], free vibration of axially loaded problems ([12] -[14]) and static bending analysis ([15],[16]), where in all these studies there are only a Winkler elastic layer linking the beams.

On the other hand, few recent works for double or multiple-beams systems resting on elastic foundations can be found in the literature. Deng et al. [17] based on Timoshenko beam theory formulate the exact dynamic stiffness matrix of the double-beam system resting on Winkler-Pasternak elastic foundation under the axial loads. Bhatra and Maheshwari [18] study the behaviour of the deformation response of rails to concentrated moving load where the Pasternak layer is used how interconnected beams layer and the foundation is of the Winkler type. Recently, Chen et al. [19] deal with the forced vibrations of a cracked double-beam system resting on Winkler-Pasternak elastic foundation based on Bernoulli-Euler beam theory. However, the studies about the DBS resting on Winkler-Kerr elastic foundations are very rare.

The current investigations is motived by to fill these gaps by studying the bending analysis of an elastically connected double-beam system resting on Winkler-Kerr foundation. A double-beam finite element (DBSWK) with ten degree of freedoms is derived and both stiffness matrix and equivalent load vector are explicitly shown. Numerical solutions of the present FEM are compared with other analytical and numerical solutions available in literature.

2 Mathematical formulation

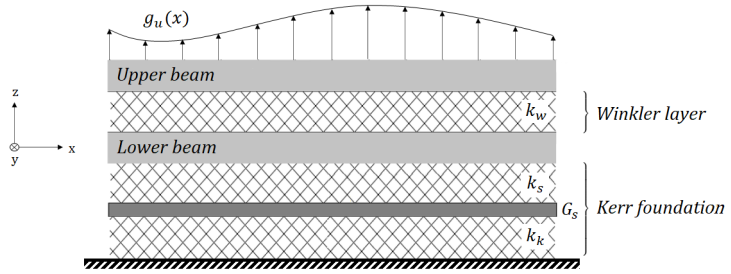

Figure 1. Double-beam system on Winkler-Kerr foundation

In this study, consider an elastically connected double-beam system resting on elastic foundation shown in the Fig. 1. This system consists of two upper and lower parallel beams assumed to be homogeneous, prismatic and of the same length L, but they can have different flexural rigidity and boundary conditions. The cinematic behavior of the cross section can be seen in Fig. 2 where its representation is based on the classical Bernoulli-Euler beam theory. The elastic connection layer between them is based on the Winkler [20] model while consist in a series of linear and independent springs with rigidity k_w where every point's reaction is proportional to the point's displacement. The elastic foundation is represented by the Kerr [21] model where three independent parameters represent the restoring force of the foundation, two linear elastic layers of constants k_c and k_k, respectively, interconnected by a unit thickness shear layer of constant G_s.

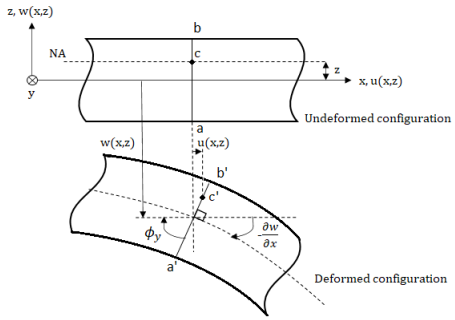

Figure 2. Cinematic of the cross section

According to Bernoulli-Euler beam theory the displacements field is given by [22]:

$$u(x,z) = z\phi_y(x), \tag{1}$$
$$w(x,z) = w(x), \tag{2}$$

where $w(x)$ denote the transverse displacement of a point on the mid plane of the beam and $\phi_y(x)$ the rotation of the cross section of the beam. According to the theory of elasticity, the strain–displacement relationships is given:

$$\varepsilon_x(x) = \frac{du(x)}{dx}, \tag{3}$$
$$\gamma_{xz}(x) = \phi_y(x) + \frac{dw(x)}{dx}, \tag{4}$$

where $\varepsilon_x(x)$ is the normal strain related to the normal stress $\sigma_x(x)$ based on the Hooke's law, and $\gamma_{xz}(x)$ is the transverse shear strains witch it is equal zero due the Bernoulli-Euler hypothesis.

The total strain energy of the elastically connected double-beam system resting Winkler-Kerr foundation, eq. (5), is composed by three parts, how can be seen as follows:

$$\Pi = \pi_b + \pi_w + \pi_k - W. \tag{5}$$

The strain energy of upper and lower beams is obtained using the kinetic relationships given on eq. (3) and eq. (4), resulting in:

$$\pi_b = \frac{1}{2}\int_0^L E_u I_u \left(w_u''(x)\right)^2 dx + \frac{1}{2}\int_0^L E_l I_l \left(w_l''(x)\right)^2 dx, \tag{6}$$

where $(') = \frac{d}{dx}$, E_u and I_u are Young's modulus and the area moment of inertia of upper beam, while E_l and I_l denote the respective properties of the lower beam, being $I = \int z^2 dA$. The Potential energy π_w induced by the Winkler elastic layer between the beams can be expressed as:

$$\pi_w = \frac{1}{2}\int_0^L k_w \left(w_u(x) - w_l(x)\right)^2 dx. \tag{7}$$

The elastic potential energy of Kerr elastic foundation π_k is denoted by:

$$\pi_k = \frac{1}{2}\int_0^L G_k \left(v'(x)\right)^2 dx + \frac{1}{2}\int_0^L k_c \left(w_l(x) - v(x)\right)^2 dx + \frac{1}{2}\int_0^L k_k v(x)^2 dx. \tag{8}$$

The work done due to transverse upper and lower load is:

$$W = \int_0^L g_u(x) w_u(x) dx + \int_0^L g_l(x) w_l(x) dx. \tag{9}$$

In order to derive the governing equation, the first variation of total strain energy eq. (5) is done:

$$\begin{aligned}
\delta\Pi \;=\; & \int_0^L \left[E_u I_u w_u'' \delta w_u'' + k_w \left(w_u - w_l\right)\delta w_u - g_u \delta w_u\right] dx + \\
& + \int_0^L \left[E_l I_l w_l'' \delta w_l'' - k_w \left(w_u - w_l\right)\delta w_l + k_c \left(w_l - v\right)\delta w_l - g_l \delta w_l\right] dx + \\
& + \int_0^L \left[G_k v' \delta v' - k_c \left(w_l - v\right)\delta v + k_k v \delta v\right] dx = 0.
\end{aligned} \tag{10}$$

Thus, the governing equations of an elastically connected Bernoulli-Euler double-beam system resting on Winkler-Kerr foundation under static loading can be written as follow:

$$E_u I_u w_u'''' + k_w \left(w_u - w_l\right) - g_u = 0, \tag{11}$$

$$E_l I_l w_l'''' - k_w \left(w_u - w_l\right) + k_c \left(w_l - v\right) - g_l = 0, \tag{12}$$

$$-G_k v'' - k_c \left(w_l - v\right) + k_k v = 0. \tag{13}$$

2.1 Finite element formulation

The variational statement in eq. (5) requires that the transverse displacement w_u and w_l, of the upper and lower beam, respectively, be three times differentiable and C^3-continuous, whereas the transverse shear layer displacement v must be once differentiable and C^1-continuous. Thus, the beams displacements are expressed as a third order polynomial equation similarly to the Finite Element approach of an isolated (without elastic foundation) Bernoulli-Euler beam, how it can be seen as follows [23]:

$$w_u(x) \;=\; a_0 + a_1 x + a_2 x^2 + a_3 x^3, \tag{14}$$

$$w_l(x) \;=\; a_0 + a_1 x + a_2 x^2 + a_3 x^3, \tag{15}$$

and the shear layer displacement given as a linear polynomial equation [24]:

$$v(x) \;=\; b_0 + b_1 x. \tag{16}$$

Thus, the interpolation functions for the ten DOF DBSWK element, shown in Fig. 3, are given by:

$$w_u(\xi) \;=\; \left[N_u(\xi)\right]\left\{u(\xi)\right\}, \tag{17}$$

$$w_l(\xi) \;=\; \left[N_l(\xi)\right]\left\{u(\xi)\right\}, \tag{18}$$

$$v(\xi) \;=\; \left[N_v(\xi)\right]\left\{u(\xi)\right\}, \tag{19}$$

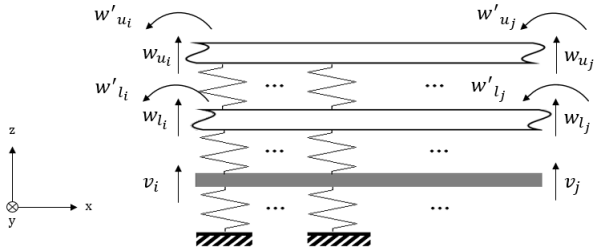

Figure 3. DBSWK finite element degrees of freedom

where the displacements and slopes at the nodes $u(\xi) = \left\{ w_{u_i}\ v_i\ w_{l_i}\ w'_{u_i}\ w'_{l_i}\ w_{u_j}\ v_j\ w_{l_j}\ w'_{u_j}\ w'_{l_j} \right\}^T$ to which the index i and j refer the initial and final nodes, respectively, and the shape functions $[N_u(\xi)] = [N_1\ 0\ 0\ N_2\ 0\ N_3\ 0\ 0\ N_4\ 0]$ and $[N_l(\xi)] = [0\ 0\ N_1\ 0\ N_2\ 0\ 0\ N_3\ 0\ N_4]$ are

$$N_1 = \frac{1}{4}(\xi-1)^2(\xi+2), \tag{20}$$

$$N_2 = \frac{L}{8}(\xi-1)^2(\xi+1), \tag{21}$$

$$N_3 = -\frac{1}{4}(\xi+1)^2(\xi-2), \tag{22}$$

$$N_4 = \frac{L}{8}(\xi+1)^2(\xi-1), \tag{23}$$

and $[N_v(\xi)] = [0\ M_1\ 0\ 0\ 0\ 0\ M_2\ 0\ 0\ 0]$ is

$$M_1 = \frac{1}{2}(1+\xi), \tag{24}$$

$$M_2 = \frac{1}{2}(1-\xi), \tag{25}$$

where a nondimensional parameter $\xi = 2x/L$ with $-1 \leq \xi \leq 1$. The distributed loading of the upper and lower beams can be interpolated by:

$$g_u(\xi) = [M_u(\xi)] \begin{Bmatrix} g_i^u \\ g_j^u \end{Bmatrix}, \tag{26}$$

$$g_l(\xi) = [M_l(\xi)] \begin{Bmatrix} g_i^l \\ g_j^l \end{Bmatrix}. \tag{27}$$

Inserting the interpolation functions, eqs. (17), (18), (19), (26) and (27) into the total strain energy eq. (5), gives the discretized form as follows:

$$\begin{aligned}
\Pi = {} & \frac{1}{2}\int_{-1}^{1} E_u I_u \left([B_u(\xi)]\{u(\xi)\}\right)^2 Jd\xi + \frac{1}{2}\int_{-1}^{1} E_l I_l \left([B_l(\xi)]\{u(\xi)\}\right)^2 Jd\xi + \\
& + \frac{1}{2}\int_{-1}^{1} k_w \left([N_u(\xi)]\{u(\xi)\} - [N_l(\xi)]\{u(\xi)\}\right)^2 Jd\xi + \frac{1}{2}\int_{-1}^{1} G_k \left([P_v(\xi)]\{u(\xi)\}\right)^2 Jd\xi + \\
& + \frac{1}{2}\int_{-1}^{1} k_c \left([N_l(\xi)]\{u(\xi)\} - [N_v(\xi)]\{u(\xi)\}\right)^2 Jd\xi + \frac{1}{2}\int_{-1}^{1} k_k \left([N_v(\xi)]\{u(\xi)\}\right)^2 Jd\xi + \\
& - \int_{-1}^{1} [M_u(\xi)]\{g^u\}[N_u(\xi)]\{u(\xi)\} Jd\xi - \int_{-1}^{1} [M_l(\xi)]\{g^l\}[N_l(\xi)]\{u(\xi)\} Jd\xi,
\end{aligned} \tag{28}$$

where $[B_u] = \left(d^2[N_u]/d\xi^2\right)\left(d^2\xi/dx^2\right)$, $[B_l] = \left(d^2[N_l]/d\xi^2\right)\left(d^2\xi/dx^2\right)$ and $[P_v] = \left(d[N_v]/d\xi\right)(d\xi/dx)$. The minimization of the discretized total energy, $\delta\Pi u = 0$, can be written as follows:

$$\delta\Pi u = \frac{1}{2}\int_{-1}^{1} \{\delta u\}^T [B_u]^T E_u I_u [B_u]\{u\} Jd\xi + \frac{1}{2}\int_{-1}^{1} \{\delta u\}^T [B_l]^T E_l I_l [B_l]\{u\} Jd\xi +$$

$$+\frac{1}{2}\int_{-1}^{1}\{\delta u\}^T\left([N_u]^T-[N_l]^T\right)k_w\left([N_u]-[N_l]\right)\{u\}\,Jd\xi+\frac{1}{2}\int_{-1}^{1}\{\delta u\}^T[P_v]^T\,G_k\,[P_v]\,\{u\}\,Jd\xi+$$
$$+\frac{1}{2}\int_{-1}^{1}\{\delta u\}^T\left([N_l]^T-[N_v]^T\right)k_c\left([N_l]-[N_v]\right)\{u\}\,Jd\xi+\frac{1}{2}\int_{-1}^{1}\{\delta u\}^T[N_v]^T\,k_k\,[N_v]\,\{u\}\,Jd\xi+$$
$$-\int_{-1}^{1}\{\delta u\}^T[N_u]^T[M_u]\{g^u\}\,Jd\xi-\int_{-1}^{1}\{\delta u\}^T[N_l]^T[M_l]\left\{g^l\right\}Jd\xi=0. \tag{29}$$

After evaluating the integrals in eq. (29), the double-beam Winkler-Kerr system can be represented by:

$$[K]\{u\}=\{p\}, \tag{30}$$

where the stiffness matrix $10x10$ is

$$[K]=[K_b]+[K_s], \tag{31}$$

and $\{p\}$ is the load vector. The nonzero coefficients of stiffness matrix $[K_b]$ are given by:

$$K_{b_{1,1}}=-K_{b_{1,6}}=-K_{b_{6,1}}=K_{b_{6,6}}=\frac{12}{L^3}E_uI_u, \tag{32}$$
$$K_{b_{1,4}}=K_{b_{1,9}}=K_{b_{4,1}}=-K_{b_{4,6}}=-K_{b_{6,4}}=-K_{b_{6,9}}=K_{b_{9,1}}=-K_{b_{9,6}}=\frac{6}{L^2}E_uI_u, \tag{33}$$
$$K_{b_{3,3}}=-K_{b_{3,8}}=-K_{b_{8,3}}=K_{b_{8,8}}=\frac{12}{L^3}E_lI_l, \tag{34}$$
$$K_{b_{3,5}}=K_{b_{3,10}}=K_{b_{5,3}}=-K_{b_{5,8}}=-K_{b_{8,5}}=-K_{b_{8,10}}=K_{b_{10,3}}=-K_{b_{10,8}}=\frac{6}{L^2}E_lI_l, \tag{35}$$
$$K_{b_{4,4}}=K_{b_{9,9}}=\frac{4}{L}E_uI_u, \tag{36}$$
$$K_{b_{4,9}}=K_{b_{9,4}}=\frac{2}{L}E_uI_u, \tag{37}$$
$$K_{b_{5,5}}=K_{b_{10,10}}=\frac{4}{L}E_lI_l, \tag{38}$$
$$K_{b_{5,10}}=K_{b_{10,5}}=\frac{2}{L}E_lI_l. \tag{39}$$

The stiffness matrix $[K_s]$ coefficients of the foundation are given by:

$$K_{s_{1,1}}=-K_{s_{1,3}}=-K_{s_{3,1}}=K_{s_{6,6}}=-K_{s_{6,8}}=-K_{s_{8,6}}=\frac{13k_wL}{35}, \tag{40}$$
$$K_{s_{1,4}}=-K_{s_{1,5}}=-K_{s_{3,4}}=K_{s_{4,1}}=-K_{s_{4,3}}=-K_{s_{5,1}}=-K_{s_{6,9}}=K_{s_{6,10}}=$$
$$=K_{s_{8,9}}=-K_{s_{9,6}}=K_{s_{9,8}}=K_{s_{10,6}}=\frac{11k_wL^2}{210}, \tag{41}$$
$$K_{s_{1,6}}=-K_{s_{1,8}}=-K_{s_{3,6}}=K_{s_{6,1}}=-K_{s_{6,3}}=-K_{s_{8,1}}=\frac{9k_wL}{70}, \tag{42}$$
$$K_{s_{1,9}}=-K_{s_{1,10}}=-K_{s_{3,9}}=-K_{s_{4,6}}=K_{s_{4,8}}=K_{s_{5,6}}=-K_{s_{6,4}}=K_{s_{6,5}}=K_{s_{8,4}}=$$
$$=K_{s_{9,1}}=-K_{s_{9,3}}=-K_{s_{10,1}}=-\frac{13k_wL^2}{420}, \tag{43}$$
$$K_{s_{2,2}}=K_{s_{7,7}}=\frac{L}{3}\left(k_c+k_k\right)+\frac{G}{L}, \tag{44}$$
$$K_{s_{2,3}}=K_{s_{3,2}}=K_{s_{7,8}}=K_{s_{8,7}}=-\frac{3k_cL}{20}, \tag{45}$$
$$K_{s_{2,5}}=K_{s_{5,2}}=-K_{s_{7,10}}=-K_{s_{10,7}}=-\frac{k_cL^2}{30}, \tag{46}$$
$$K_{s_{2,7}}=K_{s_{7,2}}=\frac{L}{6}\left(k_c+k_k\right)-\frac{G}{L}, \tag{47}$$
$$K_{s_{2,8}}=K_{s_{3,7}}=K_{s_{7,3}}=K_{s_{8,2}}=-\frac{7k_cL}{20}, \tag{48}$$
$$K_{s_{2,10}}=-K_{s_{5,7}}=-K_{s_{7,5}}=K_{s_{10,2}}=\frac{k_cL^2}{20}, \tag{49}$$
$$K_{s_{3,3}}=K_{s_{8,8}}=\frac{13L}{35}\left(k_c+k_w\right), \tag{50}$$

$$K_{s_{3,5}} = K_{s_{5,3}} = -K_{s_{8,10}} = -K_{s_{10,8}} = \frac{11L^2}{210}\left(k_c + k_w\right), \tag{51}$$

$$K_{s_{3,8}} = K_{s_{8,3}} = \frac{9L}{70}\left(k_c + k_w\right), \tag{52}$$

$$K_{s_{3,10}} = -K_{s_{5,8}} = -K_{s_{8,5}} = K_{s_{10,3}} = -\frac{13L^2}{420}\left(k_c + k_w\right), \tag{53}$$

$$K_{s_{4,4}} = -K_{s_{4,5}} = -K_{s_{5,4}} = K_{s_{9,9}} = -K_{s_{9,10}} = -K_{s_{10,9}} = \frac{k_w L^3}{105}, \tag{54}$$

$$K_{s_{4,9}} = -K_{s_{4,10}} = -K_{s_{5,9}} = K_{s_{9,4}} = -K_{s_{9,5}} = -K_{s_{10,4}} = -\frac{k_w L^3}{140}, \tag{55}$$

$$K_{s_{5,5}} = K_{s_{10,10}} = \frac{L^3}{105}\left(k_c + k_w\right), \tag{56}$$

$$K_{s_{5,10}} = K_{s_{10,5}} = -\frac{L^3}{140}\left(k_c + k_w\right), \tag{57}$$

and $K_{s_{1,2}} = K_{s_{1,7}} = K_{s_{2,1}} = K_{s_{2,4}} = K_{s_{2,6}} = K_{s_{2,9}} = K_{s_{4,2}} = K_{s_{4,7}} = K_{s_{6,2}} = K_{s_{6,7}} = K_{s_{7,1}} = K_{s_{7,4}} = K_{s_{7,6}} = K_{s_{7,9}} = K_{s_{9,2}} = K_{s_{9,7}} = 0$.

The load vector $\{p\}$ can be composed by distributed and concentrated loads applied under upper or/and lower beams. Therefore, the distributed linear load vector is obtained by the equation:

$$\{p_d\} = \frac{L}{60}\left[A\right]\begin{Bmatrix} g_i^u \\ g_i^l \\ g_j^u \\ g_j^l \end{Bmatrix}, \tag{58}$$

where

$$A_{1,1} = A_{3,2} = A_{6,3} = A_{8,4} = 9, \tag{59}$$

$$A_{1,3} = A_{3,4} = A_{6,1} = A_{8,2} = 21, \tag{60}$$

$$A_{4,1} = A_{5,2} = -A_{9,3} = -A_{10,4} = 2L, \tag{61}$$

$$A_{4,3} = A_{5,4} = -A_{9,1} = -A_{10,2} = 3L, \tag{62}$$

and all the remaining terms from matrix $[A]$ are null.

2.2 Numerical examples

In this section examples modelled by the finite elements having ten DOF double-beam on Kerr foundation are done and compared with the exact solution. Initially it's done a convergence test considering a simple support double-beam system in order to analyse the finite element formulation. Finally, different properties, beams ends conditions and load cases are evaluated.

Example I

Consider that the double-beam system has simply supported ends and the same properties: $E = E_u = E_l = 2 \times 10^9 kN/cm^2$, $I = I_u = I_l = 6.667 \times 10^{-5} m^4$, and $L = 10m$. In addition, the springs parameters have the same values $k = k_w = k_c = k_k = 10^3 kN/m^2$ and the transverse shear layer constant is $G_s = 10^6 kN$. A distributed uniform load act across upper beam with intensity $g_u(x) = -10kN$. The displacements and slopes results are compared with the exact solution obtained by eqs. (11), (12) and (13) expanding the displacements in a Fourier series, as follows:

$$w_u(x) = \sum_{n=1,3}^{N} \frac{4g_u}{\pi n \beta}\left(3k^2 + 2G_s k\lambda_n^2 + 2EIk\lambda_n^4 + G_s EI\lambda_n^6\right) sin\left(\lambda_n x\right), \tag{63}$$

$$w_l(x) = \sum_{n=1,3}^{N} \frac{4g_u k}{\pi n \beta}\left(2k + G_s\lambda_n^2\right) sin\left(\lambda_n x\right), \tag{64}$$

$$v(x) = \sum_{n=1,3}^{N} \frac{4g_u k^2}{\pi n \beta} sin\left(\lambda_n x\right), \tag{65}$$

where $\beta = G_s E^2 I^2 \lambda_n^{10} + 2E^2 I^2 k \lambda_n^8 + 5EIk^2 \lambda_n^4 + 3G_s EIk \lambda_n^6 + G_s k^2 \lambda_n^2 + k^3$ and $k_n = \frac{n\pi}{L}$. The slopes can be obtained deriving eq. (63) and (64) with respect to x coordinate, resulting in:

$$\frac{d}{dx}|w_u(x)| = \sum_{n=1,3}^{N} \frac{4g_u}{\pi n \beta} \left(3k^2\lambda_n + 2G_s k \lambda_n^3 + 2EIk\lambda_n^5 + G_s EI\lambda_n^7\right) cos\left(\lambda_n x\right), \tag{66}$$

$$\frac{d}{dx}|w_l(x)| = \sum_{n=1,3}^{N} \frac{4g_u k}{\pi n \beta} \left(2k\lambda_n + G_s \lambda_n^3\right) cos\left(\lambda_n x\right). \tag{67}$$

To clarify the steps involved in solving this simple example two at thirty DBSWK finite elements are used to solve the middle displacements and left ends slopes and this results are compared with the exact solution as shown in Tables 1 and 2, Fig. 4 shows the convergence of the BDSWK finite element.

Table 1. FEM and exact middle displacements comparative

DOF	2 FE	4 FE	6 FE	8 FE	10 FE	20 FE	Exact
$w_u.\left(10^3\right)$	6.3616	6.3460	6.3456	6.3456	6.3456	6.3457	6.3457
$w_l\left(10^3\right)$	1.9319	1.9387	1.9397	1.9400	1.9402	1.9404	1.9404
$v\left(10^5\right)$	1.0859	1.7264	1.8388	1.8777	1.8956	1.9194	1.9273

Table 2. FEM and exact slope left or right ends comparative

DOF	2 FE	4 FE	6 FE	8 FE	10 FE	20 FE	Exact
$w'_u.\left(10^3\right)$	2.0555	2.0502	2.0501	2.0501	2.0501	2.0501	2.0501
$w'_l.\left(10^4\right)$	6.072	6.0952	6.0983	6.0994	6.0999	6.1006	6.1008

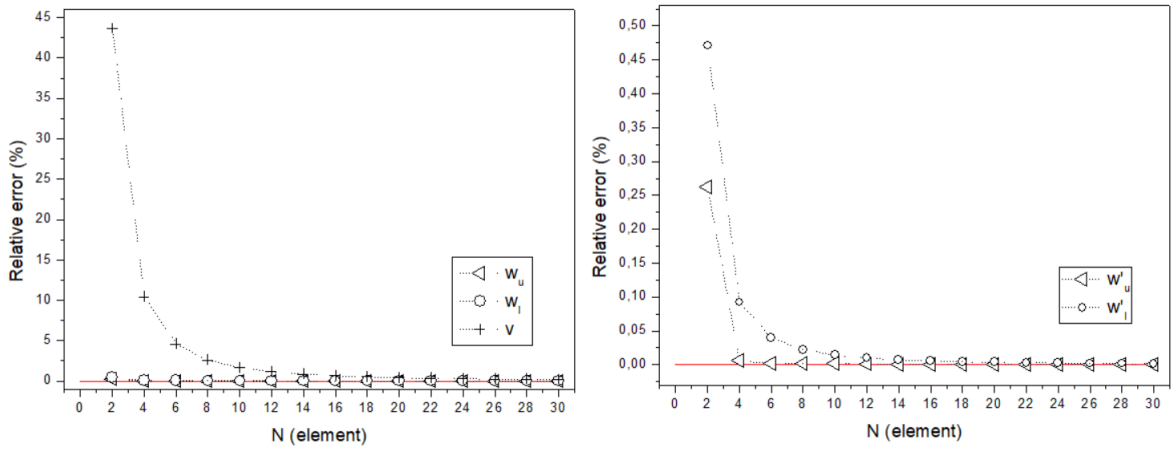

Figure 4. Relative error considering different mesh sizes

The results show that the BDSWK finite element formulation presented in this work recover the exact and the displacements and rotations converge to the analytical solution, faster to the beams and slower to the shear layer.

Example II

Consider the double-beam system having different material properties, springs rigidities and distributed loads being left ends simply supported and the right ends guide-supported, see Fig. 5. Thus, the upper beam has Young's modulus $E_u = 13 \times 10^6 kN/m^2$ and a rectangular cross section with dimensions $b_u = 0.15m$, $h_u = 1m$, while the lower beam has $E_l = 0.5E_u$ and cross section $b_l = 0.25m$ and $h_l = 1m$, and the same length $L = 100m$.

Both beams are subject to a uniformly distributed load with intensity $g_u = -10kN/m$ and $g_l = -15kN/m$. The Winkler inner layer has rigidity $k_w = 6.5 \times 10^2 kN/m^2$, and the Kerr elastic foundation parameters are: $k_c = 10^3 kN/m^2$, $k_k = 1.5 \times 10^3 kN/m^2$, and $G_s = 10^2 kN$. The exact solution can be calculated by:

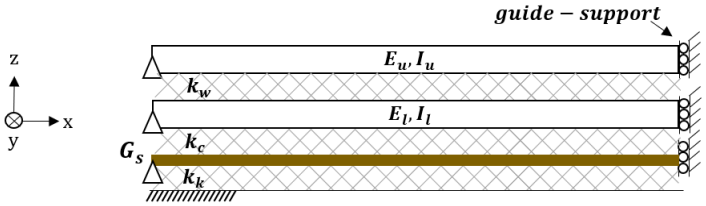

Figure 5. DBS with guide-supported right ends

$$w_u(x) = \left\{\chi_u k_c \left(G_s\lambda_n^2 + k_k\right) + \left[\left(\chi_u + \chi_l\right) k_w + \chi_u E_l I_l \lambda_n^4\right]\left(G_s\lambda_n^2 + k_c + k_k\right)\right\} sin(\lambda_n x), \quad (68)$$

$$w_l(x) = \left[\left(\chi_u + \chi_l\right) k_w + \chi_l E_u I_u \lambda_n^4\right]\left(G_s\lambda_n^2 + k_c + k_k\right) sin(\lambda_n x), \quad (69)$$

$$v(x) = \left(\left(\chi_u + \chi_l\right) k_w + \chi_l E_u I_u \lambda_n^4\right) k_c sin(\lambda_n x), \quad (70)$$

where $\lambda_n = \frac{n\pi}{2L}$, $\beta = \alpha_0\lambda^{10} + \alpha_1\lambda^8 + \alpha_2\lambda^6 + \alpha_3\lambda^4 + \alpha_4\lambda^2 + \alpha_5$, $\alpha_0 = E_u E_l I_u I_l G_s$, $\alpha_1 = E_u E_l I_u I_l \left(k_c + k_k\right)$, $\alpha_2 = G_s\left[E_u I_u k_c + k_w\left(E_u I_u + E_l I_l\right)\right]$, $\alpha_3 = E_u I_u k_c k_k + k_w\left(E_u I_u + E_l I_l\right)\left(k_c + k_k\right)$, $\alpha_4 = G_s k_c k_w$, $\alpha_6 = k_w k_c k_k$, $\chi_u = \frac{2g_u}{\beta\lambda_n L}$, and $\chi_l = \frac{2g_l}{\beta\lambda_n L}$.

The displacements on the beams and shear layer can be seen in Fig. 6 as well as the beams slopes along the length to twenty finite elements, where the results are compared with the exact solution given in eqs. (68-70) and your derivatives.

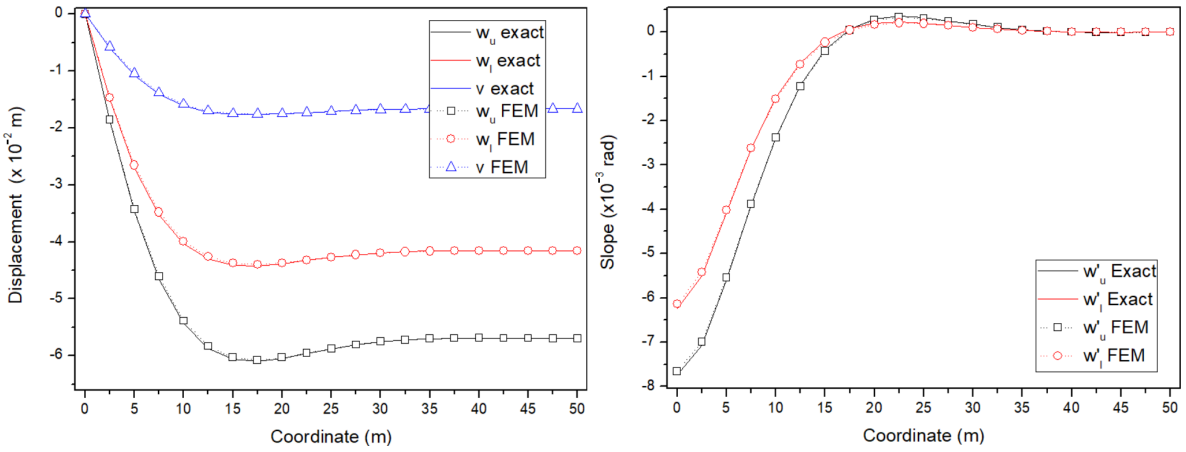

Figure 6. Displacements and slopes along beams and shear layer

Figures shows that the maximum displacements do not occur in the right ends. Table 3 shown the x coordinate related the maximum displacement and a comparative with the right ends values. Thus, the results shows that the

Table 3. Maximum and right ends displacements

Coord. (m)	$w_u(\times 10^3 m)$	Coord.(m)	$w_l(\times 10^3 m)$	Coord. (m)	$v(\times 10^3 m)$
$x = 17.00150$	6.09994	$x = 16.58275$	4.42105	$x = 16.59425$	1.76826
$x = 50.00000$	5.69652	$x = 50.00000$	4.16130	$x = 50.00000$	1.66452

FEM solution have a good performance even if having different beams and springs properties, different loads and boundary conditions when compared with the exact solution.

Example III

In this example, different boundary conditions are used and the DBSWK bahavior is valued. Therefore, consider that the properties are the same that example 2.2 and the same uniformly distributed loads. In addition, a concentrated downward load $p_l = 1000kN$ is applied on the lower beam at $x = 10m$ from the left end. Five different boundary conditions cases are done: case 1 - CSCCSC; case 2 - CSCFFF; case 3 - SFSSFS; case 4 - SFCSFF; and case 5 - FSFFSF; where C is clamped, S is simple, and F is free end. The results using twenty finite elements can be seen in Table 4 and Fig. 7 to 11.

Table 4. Displacements and slopes in the x position $(x10^{-2})$

	Coord. (m)	w_u	v	w_l	w'_u	w'_l
	$x = 0$	0	0	0	0	0
Case 1	$x = L/2$	-7.15066	-1.94841	-4.82425	0.40017	0.22045
	$x = L$	0	0	0	0	0
	$x = 0$	0	0	0	0	0
Case 2	$x = L/2$	-6.92859	-1.89522	-4.68902	0.41585	0.22976
	$x = L$	-5.79273	-1.67392	-4.21386	-0.03351	-0.01937
	$x = 0$	0	-1.25377	0	-2.35317	-2.08979
Case 3	$x = L/2$	-6.93143	-1.90298	-4.69603	0.43493	0.24134
	$x = L$	0	-0.36154	0	0.74466	0.60584
	$x = 0$	0	-0.30407	0	-1.88691	0
Case 4	$x = L/2$	-6.97912	-1.91736	-4.7361	0.41221	0.23295
	$x = L$	0	-0.81963	-1.65319	0.80892	0.26285
	$x = 0$	-8.41101	0	-3.85277	-1.12164	-1.60279
Case 5	$x = L/2$	-6.56053	-1.80813	-4.46166	0.42221	0.23326
	$x = L$	-5.35991	0	-3.68282	0.00926	0.04334

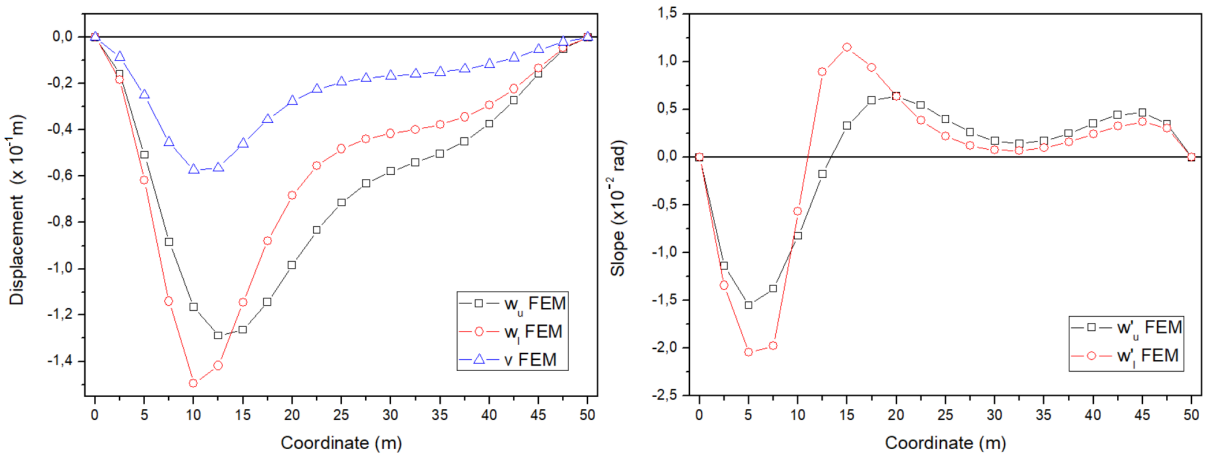

Figure 7. Displacements and slopes along the beams and shear layer considering the case 1.

One more time, the versatility of the FEM formulation presented in this paper to solve different boundary cases associated to different mechanical properties and loads could be seen. As expected, the boundary conditions directly influence the displacements and slopes of the beams and associated with the Kerr layer conduce to the interesting results once that all of these cases the displacements and rotations are very closed and this fact is associated with the reactive force produced by Kerr layer. Moreover, the excentric concentrated load applied in lower beam produce a non-uniform behavior of the system.

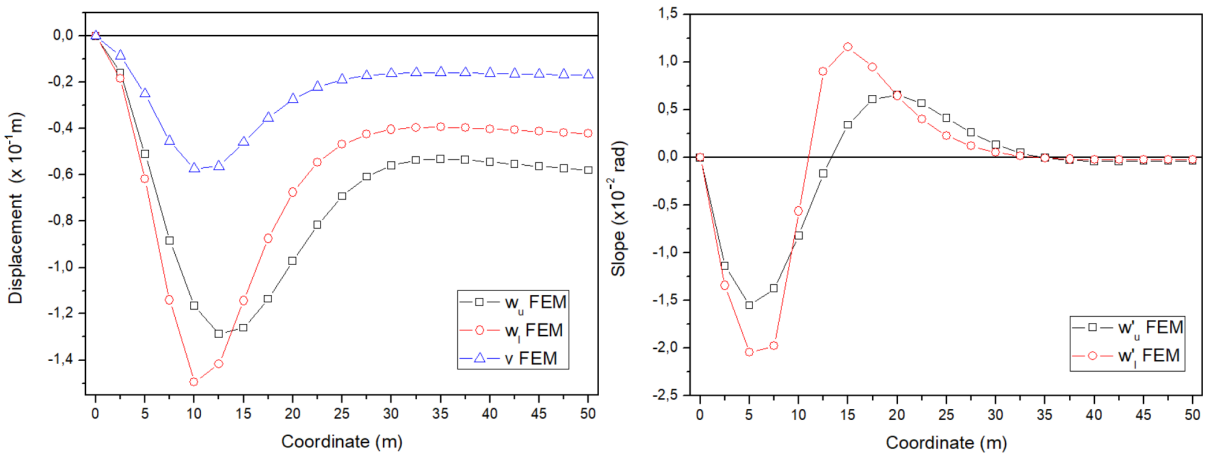

Figure 8. Displacements and slopes along the beams and shear layer considering the case 2.

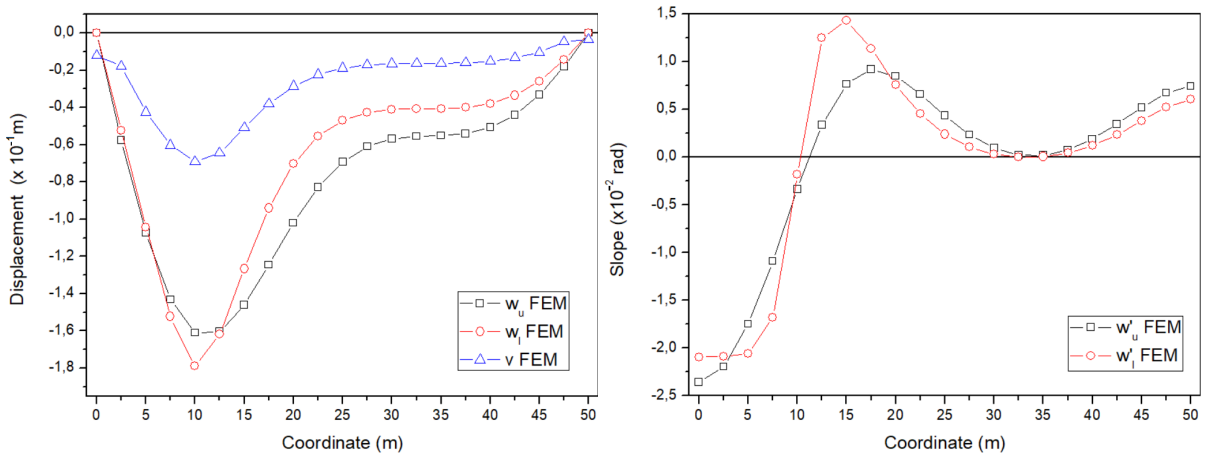

Figure 9. Displacements and slopes along the beams and shear layer considering the case 3.

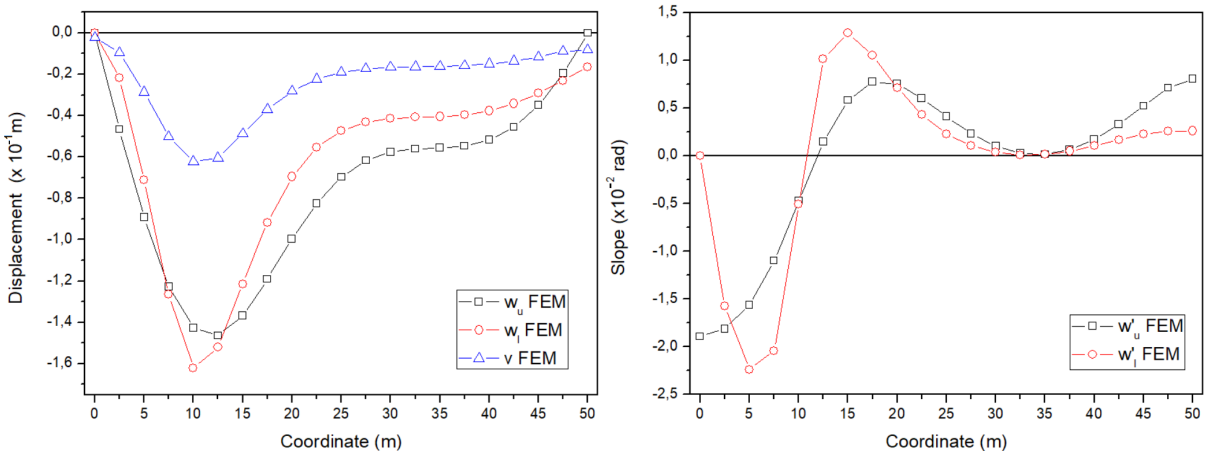

Figure 10. Displacements and slopes along the beams and shear layer considering the case 4.

3 Conclusions

In this paper a Finite Element Method formulation to bending analysis of a double-beam system resting on Kerr foundation is done. Based on the Bernoulli-Euler beam theory, a six-node finite element with ten degrees of freedom is derived and the both stiffness matrix and load vector are explicitly shown.

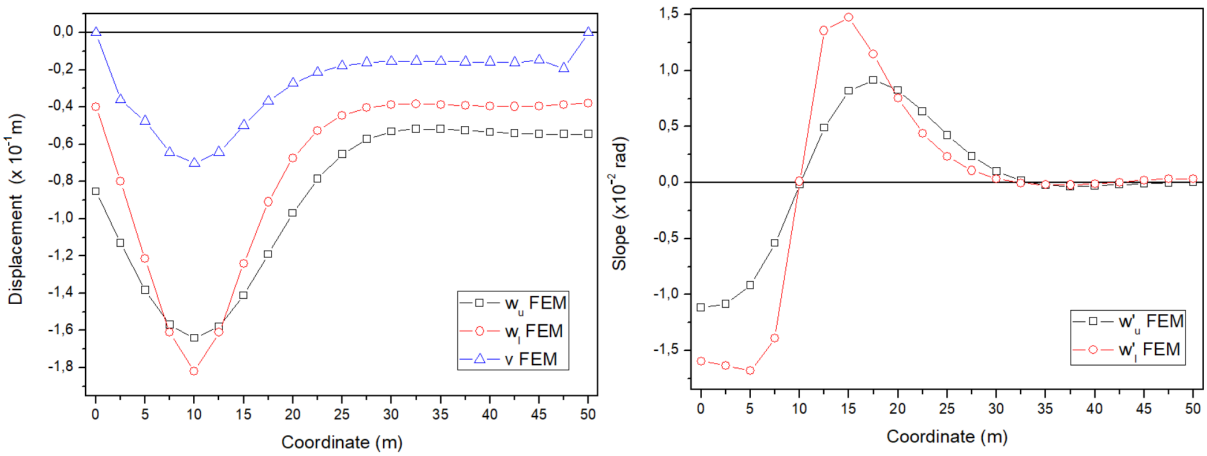

Figure 11. Displacements and slopes along the beams and shear layer considering the case 5.

The model is validated by the exact solution for two cases: in the first one, all ends are simple support and the convergence is investigated; On the second case, the left ends are simple support and the right ends are a guide-support. The results show that there are good agreements between the present results and the exact solution.

It is concluded that the formulation given in this paper is very attractive due to its versatility solving any problems considering different geometrical/mechanical properties, boundary conditions, and loading cases of the beams and shear layer.

Acknowledgements. This study was financed in part by the Coordenação de Aperfeiçoamento de Pessoal de Nível Superior – Brasil (CAPES) – Finance Code 001.

Authorship statement. The authors hereby confirm that they are the sole liable persons responsible for the authorship of this work, and that all material that has been herein included as part of the present paper is either the property (and authorship) of the authors, or has the permission of the owners to be included here.

References

[1] J. Seelig, I. Hoppmann, and others. Impact on an elastically connected double beam system. Technical report, RENSSELAER POLYTECHNIC INST TROY NY, 1963.

[2] J. Seelig and W. Hoppmann. Normal mode vibrations of systems of elastically connected parallel bars. *The Journal of the Acoustical Society of America*, vol. 36, n. 1, pp. 93–99, 1964.

[3] P. Kessel. Resonances excited in an elastically connected double-beam system by a cyclic moving load. *The Journal of the Acoustical Society of America*, vol. 40, n. 3, pp. 684–687, 1966.

[4] S. CHONAN. Dynamical behaviours of elastically connected double-beam systems subjected to an impulsive load. *Bulletin of JSME*, vol. 19, n. 132, pp. 595–603, 1976.

[5] T. R. Hamada, H. NAKAYAMA, and K. HAYASHI. Free and forced vibrations of elastically connected double-beam systems. *Bulletin of JSME*, vol. 26, n. 221, pp. 1936–1942, 1983.

[6] Z. Oniszczuk. Free transverse vibrations of elastically connected simply supported double-beam complex system. *Journal of sound and vibration*, vol. 232, n. 2, pp. 387–403, 2000.

[7] Z. Oniszczuk. Forced transverse vibrations of an elastically connected complex simply supported double-beam system. *Journal of Sound and Vibration*, vol. 264, n. 2, pp. 273–286, 2003.

[8] S. G. Kelly. Free and forced vibrations of elastically connected structures. *Advances in Acoustics and Vibration*, vol. 2010, 2010.

[9] Q. Mao. Free vibration analysis of elastically connected multiple-beams by using the adomian modified decomposition method. *Journal of Sound and Vibration*, vol. 331, n. 11, pp. 2532–2542, 2012.

[10] M. Huang and J. Liu. Substructural method for vibration analysis of the elastically connected double-beam system. *Advances in Structural Engineering*, vol. 16, n. 2, pp. 365–377, 2013.

[11] A. Mirzabeigy, R. Madoliat, and C. Surace. Explicit formula to estimate natural frequencies of a double-beam system with crack. *Journal of the Brazilian Society of Mechanical Sciences and Engineering*, vol. 41, n. 5, pp. 1–12, 2019.

[12] Y. Zhang, Y. Lu, S. Wang, and X. Liu. Vibration and buckling of a double-beam system under compressive axial loading. *Journal of Sound and Vibration*, vol. 318, n. 1-2, pp. 341–352, 2008.
[13] S. G. Kelly and S. Srinivas. Free vibrations of elastically connected stretched beams. *Journal of Sound and Vibration*, vol. 326, n. 3-5, pp. 883–893, 2009.
[14] Q. Mao and N. Wattanasakulpong. Vibration and stability of a double-beam system interconnected by an elastic foundation under conservative and nonconservative axial forces. *International Journal of Mechanical Sciences*, vol. 93, pp. 1–7, 2015.
[15] M. Chung and K. Lin. Model and analysis method for machine components in contact. In *Computational Mechanics' 88*, pp. 957–958. Springer, 1988.
[16] W. Brito, C. Maia, and A. Mendonca. Bending analysis of elastically connected euler–bernoulli double-beam system using the direct boundary element method. *Applied Mathematical Modelling*, vol. 74, pp. 387–408, 2019.
[17] H. Deng, W. Cheng, S. Zhao, and others. Vibration and buckling analysis of double-functionally graded timoshenko beam system on winkler–pasternak elastic foundation. *Composite Structures*, vol. 160, pp. 152–168, 2017.
[18] S. Bhatra and P. Maheshwari. Double beam model for reinforced tensionless foundations under moving loads. *KSCE Journal of Civil Engineering*, vol. 23, n. 4, pp. 1600–1609, 2019.
[19] B. Chen, B. Lin, X. Zhao, W. Zhu, Y. Yang, and Y. Li. Closed-form solutions for forced vibrations of a cracked double-beam system interconnected by a viscoelastic layer resting on winkler–pasternak elastic foundation. *Thin-Walled Structures*, vol. 163, pp. 107688, 2021.
[20] E. Winkler. Die lehre von der elastizität und festigkeit (the theory of elasticity and stiffness). *Prague: H. Dominius*, 1867.
[21] A. D. Kerr. A study of a new foundation model. *Acta Mechanica*, vol. 1, n. 2, pp. 135–147, 1965.
[22] C. Wang, J. N. Reddy, and K. Lee. *Shear deformable beams and plates: Relationships with classical solutions*. Elsevier, 2000.
[23] M. Petyt. *Introduction to finite element vibration analysis*. Cambridge university press, 2010.
[24] L. M. Antonio, R. Pavanello, and de P. L. Almeida Barros. Marine pipeline–seabed interaction modeling based on kerr-type foundation. *Applied ocean research*, vol. 80, pp. 228–239, 2018.